Reduction and Analysis of Networks of Nonlinear Oscillators under Weak Coupling Gain

Anes Lazri, Antonio Loria, Elena Panteley

Reduction and Analysis of Networks of Nonlinear Oscillators under Weak Coupling Gain

Anes Lazri Elena Panteley Antonio Loría

***Abstract*— We analyze the behavior of Stuart-Landau oscillator networks interconnected with low coupling gain. It is known in the literature that when the coupling gain is sufficiently high, full synchronization takes place between the different oscillators in the network. In this paper, we are interested in the case where the coupling gain is not sufficiently high, we propose a method for reducing the network using the spectral properties of the Laplacian, which can then be used to analyze the possible exhibited behaviors. Secondly, and still in order to analyze the network's behavior via the proposed reduced model, we analyze the effect of an oscillation frequency perturbation in the first oscillator on the network as a whole.**

I. Introduction

This paper focuses on the synchronization of Stuart-Landau oscillator networks, which represent a generic model of nonlinear oscillators near a Hopf bifurcation [1], [2], [3], [4]. Stuart-Landau oscillators, which are often used to represent lasers [5], neuronal networks [6], [7], and various biological systems [8], *etc.*, are also known for the very rich behaviors they can exhibit, depending on their own parameters as well as those related to coupling. This richness can be seen even when the network contains only two oscillators—see [1].

One of the widely observed behaviors of oscillator networks is *dynamic consensus*, which consists of the total synchronization into an averaged oscillator [9]. This behavior is only possible when the coupling gain is relatively high. On the contrary, when the coupling gain is low, clustering takes place. In other words, subgroups of oscillators synchronize with each other but not with the other oscillators in the network, even if they are not directly connected (remote synchronization —see , *e.g.*, [6],[7], [10]). This behavior is highlighted in [11] for a network of oscillators interconnected on a Stuart-Landau topology. As explained in [12] and [13], this particular behavior is linked to the structure of the interconnection graph and the coupling gain. In order to explain the different behaviors when the coupling gain is relatively low, the authors of [11] present a bifurcation analysis via linearization of dynamics. However, it is strongly believed that it is possible to analyze the network synchronization problem via graph reduction.

Reducing the dynamics of interconnected Stuart-Landau oscillators has been investigated in the literature. Indeed, in [14], a technique to reduce the network, by considering the parameters and spectral properties of the matrices linked to the interconnection graph, is presented. However, the reduced-order network model obtained by the method proposed in [14] has *nonlinear* interconnections. This hampers significantly the analysis of the reduced-order network, let alone, the characterization of the various possible behaviors, in function of the coupling gain.

For a network of connected Stuart-Landau oscillators with relatively high coupling gain, the authors of [9] approximate the general behavior of the network by a single averaged oscillator; this makes sense given that the behavior that emerges is that of a single oscillator. This work, as well as [14], motivates our work. One of the aims is to present a reduced model with linear interconnections, that we can analyze the various possible behaviors for the network under consideration.

As far as we know, apart from [14], eigenvectors-based graph-reduction methods have not yet been applied to nonlinear oscillators. Furthermore, given that Stuart-Landau oscillators are represented by a complex variable model, many works in the literature have focused on cases in which the interconnection gain is not scalar [1], [10], [4]. In these papers, the authors explain the possible behaviors of oscillators, which are rich and strongly dependent on the values of the interconnection gain. That said, it is interesting to apply a graph reduction method on a network where the coupling gain is not scalar.

It is also worth noting that when the coupling is relatively high, full synchronization of the oscillators takes place. Nevertheless, the effect of a perturbation on the frequency of one of the oscillators may completely change the emergent behavior —see [15], [16]. Depending on the value of the disturbance, we may see an oscillation death, a phase lock, or even a phase drift. This problem is addressed in [11] for identical interconnected oscillators on a star network when the frequency of the central node is disturbed. This is also studied for a heterogeneous network in [17] considering more considerable disturbances. In this paper, after proposing a reduced model, we use this model to analyze the various possible behaviors of the network when a frequency disturbance is introduced.

To be more precise, we use the spectral properties of the network's Laplacian to perform a graph reduction. Most notably, we show that the systems constituting the reduced network are Stuart-Landau oscillators linked together through diffusive complex connections. Subsequently, we investigate how a perturbation in frequency affects the overall system behavior when the coupling is scalar, using this reduced-

A. Lazri is with laboratoire des signaux et systèmes (L2S), CNRS, Univ Paris-Saclay, France (e-mail: anes.lazri@centralesupelec.fr) E. Panteley and A. Loría are with L2S, CNRS, (e-mail: {elena.panteley,antonio.loria}@cnrs.fr).

order network. Similar to the approaches in [11] and [14], our analysis is limited to network structures with specific structural criteria. It is worth noting that, to the best of our knowledge, the general problem of graph reduction that preserves the interconnection nature (diffusive, direct...) remains open for networks of nonlinear systems.

II. Problem Formulation

Consider a network of N Stuart-Landau oscillators,

$$\dot{z}_k = -z_k|z_k|^2 + (\alpha + i\omega)z_k + u_k, \qquad k \leq N \tag{1}$$

where α is a parameter detarmining the rate of convergence of trajectories towards the the attractor, ω is the natural frequency of oscillation, and the state $z_k \in \mathbb{C}$ has a representation on the Cartesian plane, given by its real part, denoted x_k, and its imaginary part y_k. We assume that the network units are connected via diffusive coupling over an undirected and connected graph. For the ith unit the coupling u_k is given by

$$u_k = -\beta \sum_{j=1}^{N} a_{ij}(\kappa z_k - z_j) \tag{2}$$

where $\beta := \gamma + i\mu \in \mathbb{C}$, with γ and $\mu > 0$, corresponds to the coupling gain, and $\kappa \in [0\,,1]$ is a coupling parameter. When $\kappa = 1$ the coupling is said to be diffusive, while the case in which $\kappa = 0$ corresponds to that of direct coupling. On the other hand, as is customary in graph theory, The weights of the interconnections amongst the nodes define the adjacency matrix, $\mathcal{A} := [a_{ij}]_{i,j\in\{1,2,\cdots,N\}}$, as well as the Laplacian matrix $L := \big[l_{ij}\big]$, where

$$l_{ij} = \begin{cases} -a_{ij} & \text{if} \quad i \neq j \\ \sum_{\substack{i=1 \\ i\neq j}}^{N} a_{ij} & \text{if} \quad i = j. \end{cases}$$

We are interested in the possible synchronized behavior of oscillators as defined above under the effect of the coupling term (2). Now, the collective behavior here mainly depends on two factors: the network's topology and the coupling gain β. For instance, for networks of identical oscillators with an underlying undirected connected-graph topology interconnected with a scalar coupling gain $\gamma > 0$ sufficiently large, the trajectories of the networked system converge to the solution of the dynamical system,

$$\dot{z}_m = -z_m|z_m|^2 + (\alpha_m + i\omega_m)z_m, \qquad i := \sqrt{-1}, \tag{3}$$

which is an emergent oscillator of the same nature—cf [9].

The behavior is much more complex when the scalar coupling gain is not large enough. From [14], it is observed that clusters emerge in this case, considering identical oscillators. As a result, such rich behavior cannot be captured by a single oscillator as defined in (3). Thus, it is necessary to represent this behavior by a reduced network.

The contribution of this paper is twofold. First, we analyze the behavior of interconnected oscillators with complex coupling gain. We show that the reduced model's dimension depends on the coupling strength's magnitude β relative to the eigenvalues of the Laplacian matrix L. Significantly, and in contrast to [14], we propose a reduced-order network with linear interconnections. Then, this reduced model elucidates the various possible network behaviors, in function of the coupling gain and the systems' parameters' values α and ω. Secondly, the reduced-order model is used to analyze the phenomenon of frequency mismatches and the impact of the latter on the synchronization problem, which supports the interest of such a model reduction.

III. Model description

Let

$$z := \begin{bmatrix} z_1 \\ z_2 \\ \vdots \\ z_N \end{bmatrix}, \qquad F(z) := \begin{bmatrix} f(z_1) \\ f(z_2) \\ \vdots \\ f(z_N) \end{bmatrix}, \tag{4}$$

where $f(z_k) = -z_k|z_k|^2$. With this notation, the diffusive coupling inputs u_k, defined in (2), can be re-written in the compact form $u = -\beta L z$. Hence, the network dynamics become

$$\dot{z} = F(z) + \Gamma z - \bar{\beta} L z, \tag{5}$$

where $\Gamma \in \mathbb{R}^{N\times N}$ corresponds to the diagonal matrix

$$\Gamma := (\tilde{\alpha} + i\tilde{\omega})I_N,$$

where $\tilde{\alpha} = \alpha + \gamma(1-\kappa)$ and $\tilde{\omega} = \omega + \mu(1-\kappa)$. Now, given the complexity of characterizing the collective emergent behavior and multi-agent synchronization for heterogeneous systems interconnected over generic graphs, even when the coupling is scalar (*i.e.* $\mu = 0$), we focus on networked systems with underlying graphs satisfying the following hypothesis.

Assumption 1: The eigenvalues $\lambda_k(L)$ of the Laplacian L and their associated eigenvectors v_k are such that:

$$\lambda_1(L) = 0 < \lambda_2(L) < \lambda_3(L) \leq \cdots \leq \lambda_N(L),$$

$$v_1 = \begin{bmatrix} 1 \\ 1 \\ \vdots \\ 1 \end{bmatrix}, \qquad \text{and} \quad v_2 = \begin{bmatrix} -1 \\ 1 \\ \vdots \\ 1 \end{bmatrix}. \tag{6}$$

□

Remark 1: We stress that many networks with weighted links satisfy Assumption 1. This class of networks contains, for example, weighted all-to-all networks and weighted grid networks. These networks are generally used to represent the behavior of brain neurons—see, *e.g.,* [18]–[20]. Multipartite graphs can also satisfy this assumption; an example is given in the simulations section. The latter find several applications in biology as for example in the analysis of the transmission of sexual disease [21] and ethnobiology [22]. It is also important to note that the Laplacian matrices of other networks can have these eigenvectors, as in the case of star networks, which are studied in depth in the literature —see [11], [23], [24].

IV. Reduced-order network and synchronization error

The determination of the order of the reduced network N_R is inherently connected to the spectral characteristics of the linear component in (5). To make this clear, it is advantageous to rewrite (5) as

$$\dot{z} = F(z) + \beta \tilde{L} z, \tag{7}$$

where $\tilde{L} := \left[-L + \frac{\beta^*}{|\beta|^2}\Gamma \right]$.

The main idea behind reducing the graph is to exploit the spectral properties of the linear part of the dynamics (7).

For the system $\dot{z} = \beta \tilde{L} z$, the eigenvalues with positive real parts in $\tilde{L}$ generate unstable modes. In contrast, those with negative real parts generate stable ones. That is, the solution to $\dot{z} = \beta \tilde{L} z$ takes the form

$$z(t) = \beta[v_1 v_{l1}^\top z(t) + v_2 v_{l2} z(t) + \cdots + v_{N_R} v_{lN_R} z(t)] + e(t),$$

where v_k and v_{lk}, for all $k \in \{1, 2, \ldots, M\}$, are respectively the right and the left eigenvectors of $\tilde{L}$ associated with the M positive real part eigenvalues of $\tilde{L}$. On the other hand, $e(t)$ contains the contributions to the solution generated by the stable modes. As $e(t) \to 0$, only the contributions of the unstable modes remain. The number of positive real part eigenvalues M defines, therefore, the order N_R of the reduced order network, and the unstable modes determine the asymptotic behavior of the network.

First, we observe that because the graph is connected, L has a unique zero eigenvalue and admits the Jordan decomposition

$$L = V \begin{bmatrix} 0 & 0 \\ 0 & \Omega_2 \end{bmatrix} V^{-1}. \tag{8}$$

Furthermore, $\Omega_2 \in \mathbb{R}^{N-1 \times N-1}$ is a diagonal matrix whose elements correspond to the nonzero eigenvalues of L. Then, in view of its definition, $\tilde{L}$ satisfies the same decomposition as L. That is, denoting by $\lambda_k(L)$ the eigenvalues of L, after (8), for all $k \in \{1, 2, \ldots, N\}$, we have

$$V^{-1} \tilde{L} V = \text{blkdiag}\left\{ \frac{\beta^*}{|\beta|^2}(\tilde{\alpha} + i\tilde{\omega}) - \lambda_k(L) \right\}. \tag{9}$$

Clearly, the number of eigenvalues of the matrix above with a positive real part varies from 1 to N depending on the value of $\beta = \gamma + i\mu$. The real part of each eigenvalue, for all $k \in \{1, 2, \ldots, N\}$, can be written as

$$Re\{\lambda_k(\tilde{L})\} = \frac{\alpha\gamma + \omega\mu}{\gamma^2 + \mu^2} - \lambda_k(L) + 1 - \kappa. \tag{10}$$

In what follows, for (α, ω) given, we are interested in the sign of the real part of the eigenvalues of $\tilde{L}$. It is observable from (10) that the number of eigenvalues with positive real part increases when $|\beta| = \sqrt{\gamma^2 + \mu^2}$ decreases. In other words, when $|\beta|$ is relatively high, only the real part of the first eigenvalue, *i.e.,* $Re\{\lambda_0(\tilde{L})\} = \frac{\alpha\gamma + \omega\mu}{\gamma^2 + \mu^2}$, is positive. On the other hand, when $|\beta|$ is relatively low, the number of positive real part eigenvalues N_R increases.

Consequently, for what follows, we set

$$\gamma_m := \frac{\alpha}{\lambda_3(L) - (1 - \kappa)} \quad \text{and} \quad \mu_m := \frac{\omega}{\lambda_3(L) - (1 - \kappa)},$$

such that $\forall \gamma > \gamma_m$ and $\mu > \mu_m$, the number of eigenvalues with positive real parts is $N_R \leq 2$. To highlight the results, the paper focuses on the case where $N_R = 2$. Prior knowledge of the graph structure under study is important for dynamics reduction since this reduction is based on the spectral properties of the graph's Laplacian. Thus, for $\gamma > \gamma_m$ and $\mu > \mu_m$, the eigenvectors associated with eigenvalues having positive real parts are v_1 and v_2 from Assumption 1. Therefore, these eigenvactoes are used to project the dynamics onto the subspace corresponding to the unstable eigenvalues of the linear part of the network dynamics.

Following this train of thought, we unfold a natural definition of the synchronization errors e. Let $V = [V_1 \ V_2]$, where $V_1 \in \mathbb{R}^{N \times N_R}$ gathers the eigenvectors associated to the N_R eigenvalues with positive real part in Eq. (8) and $V_2 \in \mathbb{R}^{N \times (N - N_R)}$ contains the remaining $N - N_R$ eigenvectors of L. Then,

$$V^{-1} = \begin{bmatrix} V_1^\dagger \\ V_2^\dagger \end{bmatrix}.$$

Next, we use V_1 and V_2 to introduce the new coordinate $\bar{z} = V^{-1} z$, and we use the partition

$$\bar{z} := \begin{bmatrix} \xi_1 \\ \xi_2 \end{bmatrix} := \begin{bmatrix} V_1^\dagger z \\ V_2^\dagger z \end{bmatrix}, \tag{11}$$

with $\xi_1 \in \mathbb{R}^{N_R}$, $\xi_2 \in \mathbb{R}^{N - N_R}$. Using $VV^{-1} = V_1 V_1^\dagger + V_2 V_2^\dagger = I_N$ we deduce the relation

$$V_2 \xi_2 = z - V_1 \xi_1, \tag{12}$$

which is useful to define the synchronization errors $e := V_2 \xi_2$, as

$$e = z - V_1 \xi_1. \tag{13}$$

It is clear from the last equation that the subspace of ξ_1 captures the generalized solutions, while the subspace of ξ_2 corresponds to a projection of the space of synchronization errors. In other words, if $e = 0$, then $\xi_2 = 0$ and $z = V_1 \xi_1$. Consequently, for $N_R = 2$, we have $V_1 = [v_1 \, v_2]$ and $V_1^\dagger = [v_{l1}^\top \, v_{l2}^\top]$, so e takes the form

$$e = z - v_1 v_{l1}^\top z - v_2 v_{l2}^\top z. \tag{14}$$

This definition of e covers the cases treated previously in the literature where the emerging dynamic is assimilated to a single system — see *e.g.* [25]. Explicitly, (14) yields

$$e = z - \begin{bmatrix} 1 & \mathbf{0}_K^\top \\ \mathbf{0}_K & \frac{1}{K}\mathbf{1}_K \mathbf{1}_K^\top \end{bmatrix} z,$$

where $\mathbf{1}_K$ is a vector of ones of size K and $\mathbf{0}_K$ a vector of size $K = N - 1$ where all entries are equal to zero. With this definition of e, we see that on $\{e = 0\}$, z_1 is unchanged and, for each $i \in \{2, 3, \cdots, N\}$, z_k converges to the average of the latter.

With this definition of e, we see that on $\{e = 0\}$, z_1 is unchanged and, for each $i \in \{2, 3, \cdots, N\}$, z_k converges to the average of the latter. Hence, defining $z_R = \left[z_1^\top \ z_2^\top \right]^\top$ as the state of the reduced order network, on $\{e = 0\}$, we have

$$z_R = W^\top z, \quad z = Q z_R \tag{15}$$

where

$$W^\top := \begin{bmatrix} 1 & 0 & 0 & \cdots & 0 \\ 0 & \frac{1}{K} & \frac{1}{K} & \cdots & \frac{1}{K} \end{bmatrix} \quad Q^\top := \begin{bmatrix} 1 & 0 & \cdots & 0 \\ 0 & 1 & \cdots & 1 \end{bmatrix}.$$

Thus, on the synchronization manifold $\{e = 0\}$, we have $z_2 = z_3 = \cdots = z_N = \frac{1}{K}\sum_{k=2}^{N} z_k$ and the dynamics described by the state $z_R = \begin{bmatrix} z_1 & z_2 \end{bmatrix}^\top = \begin{bmatrix} z_1 & \frac{1}{K}\sum_{k=2}^{N} z_k \end{bmatrix}^\top$ persist asymptotically.

We are ready to present our first statements: Proposition 1 on the dynamics of the synchronization errors e and Proposition 2 on the reduced-order network, with state z_R.

Proposition 1 (synchronization): For a network of systems with dynamics (1) in closed loop with (2), under Assumption 1, the set $\{e = 0\}$, where e is defined in (14), is globally exponentially stable, for any $\beta > \beta_m := \gamma_m + i\mu_m$. □

Proof: After (11) and (12), we have $e = V_2 V_2^\dagger z$. Now, consider the Lyapunov function candidate $\mathcal{V}(e) = \frac{1}{2}\|e\|^2 = \frac{1}{2}e^* e$, where e^* is the conjugate transpose of the vector e. Furthermore, let $P := V_2 V_2^\dagger = I_N - V_1 V_1^\dagger$. Clearly, $P = P^\top$ and $P^\top P = P$. Moreover,

$$\mathcal{V}(e) \equiv \mathcal{V}_z(z) := \frac{1}{2} z^* P z. \tag{16}$$

Therefore, the total derivative of $V(e)$ may be computed by differentiating $V_z(z)$ above, along the trajectories of (7). For clarity, we split $\dot{V}_z(z)$ into

$$\dot{\mathcal{V}}_z(z) := \dot{\mathcal{V}}_z^{(l)}(z) + \dot{\mathcal{V}}_z^{(nl)}(z),$$

where

$$\dot{\mathcal{V}}_z^{(l)}(z) := \frac{\partial \mathcal{V}_z^{(l)}}{\partial z} \beta \tilde{L} z, \tag{17}$$

$$\dot{\mathcal{V}}_z^{(nl)}(z) := \frac{\partial \mathcal{V}_z^{(nl)}}{\partial z^\top} F(z), \tag{18}$$

and we compute $\dot{V}_z^{(l)}(z)$ and $\dot{V}_z^{(nl)}(z)$ separately. For the former, we use the identity $e = Pz$, to obtain

$$\dot{\mathcal{V}}^{(l)}(e) = \frac{\beta}{2} e^* P \tilde{L} z + \frac{\beta^*}{2} z^\top \tilde{L}^\top P e. \tag{19}$$

Next, since $V = [V_1\ V_2]$, $P = V_2 V_2^\dagger$ is equivalent to

$$P = V \begin{bmatrix} 0 & 0 \\ 0 & I_{N-N_R} \end{bmatrix} V^{-1}. \tag{20}$$

On the other hand, for $N_R = 2$, we have

$$\tilde{L} = V \begin{bmatrix} \Lambda_1 & 0 \\ 0 & \Lambda_2 \end{bmatrix} V^{-1}, \tag{21}$$

where $\Lambda_2 \in \mathbb{R}^{(N-N_R)\times(N-N_R)}$ is a block diagonal matrix gathering $N - N_R$ blocks with negative-real-part eigenvalues $\lambda_k(\tilde{L})$.

Therefore, using (20) and (21) in (19), we obtain

$$\dot{\mathcal{V}}^{(l)}(e) = \frac{\beta}{2} e^* V \begin{bmatrix} 0 & 0 \\ 0 & \Lambda_2 \end{bmatrix} V^{-1} z + \frac{\beta^*}{2} z^\top \left[V \begin{bmatrix} 0 & 0 \\ 0 & \Lambda_2^\top \end{bmatrix} V^{-1} \right]^\top e,$$

or, equivalently,

$$\dot{\mathcal{V}}^{l}(e) = \frac{\beta}{2} e^* V_2 \Lambda V_2^\dagger z + \frac{\beta}{2} z^\top \left[V_2 \Lambda V_2^\dagger \right]^\top e.$$

Now, since $V_2^\dagger V_2 = I_{N-N_R}$, we have $V_2^\dagger e = V_2^\dagger z$, so

$$\dot{\mathcal{V}}^{(l)}(e) = \frac{\beta + \beta^*}{2} e^* V_2 \left[\Lambda + \Lambda^\top\right] V_2^\dagger e.$$

Finally, since $\left[\Lambda + \Lambda^\top\right]$ is a diagonal matrix with $N - N_R$ entries with negative real part,

$$\dot{\mathcal{V}}^{(l)}(e) \leq \frac{\beta + \beta^*}{2} \Re e\{\lambda_3(\tilde{L})\} ||e||^2, \tag{22}$$

where $\lambda_3(\tilde{L})$ is the lowest eigenvalue of $\tilde{L}$ with negative real part. Now we focus on $\dot{V}_z^{(nl)}(z)$ and show that it is non-positive. To that end, we develop the matrix product on the right-hand side of (16) to obtain

$$\mathcal{V}_z(z) = \frac{1}{2K} \sum_{k=2}^{N} \sum_{j=2}^{N} ||z_k - z_j||^2. \tag{23}$$

The total derivative of the latter along the trajectories of (1) and disregarding the linear terms (including the inputs), yields

$$\dot{\mathcal{V}}_z^{(nl)}(z) = \frac{1}{K} \sum_{k=2}^{N} \sum_{j=2}^{N} -|z_k|^4 - |z_j|^2 + z_k^* z_j |z_j|^2 + z_j^* z_k |z_k|^2.$$

However, for each $\{i, j\} \in \{2, 3, \cdots, N\}$,

$$|z_k|^2 z_k z_j^* + |z_j|^2 z_j z_k^* \leq \frac{1}{2}|z_k|^4 + |z_k|^2|z_j|^2 + \frac{1}{2}|z_j|^4.$$

Hence,

$$\begin{aligned} \dot{\mathcal{V}}_z^{(nl)}(z) &\leq \frac{1}{K} \sum_{k=2}^{N} \sum_{j=2}^{N} -\frac{1}{2}|z_k|^4 + |z_k|^2|z_j|^2 - \frac{1}{2}|z_j|^4 \\ &\leq -\frac{1}{2K} \sum_{k=2}^{N} \sum_{j=2}^{N} (|z_k|^2 - |z_j|^2)^2. \end{aligned}$$

Thus,

$$\dot{\mathcal{V}}_z^{(nl)}(z) \leq 0. \tag{24}$$

Putting together (24) and (22), and in view of the first identity in (16), we obtain

$$\dot{\mathcal{V}}(e) \leq \gamma \Re e\{\lambda_3(\tilde{L})\} ||e||^2.$$

Since $\lambda_3(\tilde{L}) < 0$, Global exponential stability of $\{e = 0\}$ follows. ■

Proposition 2 (reduced-order network): Consider a network of N Stuart-Landau oscillators with dynamics (1), in closed-loop with (2) and under Assumption 1. Then, on the synchronization manifold $\{e = 0\}$, if $\beta > \beta_m = \gamma_m + i\mu_m$, there exists a network of reduced order $N_R = 2$, whose nodes are dynamical systems of the form

$$\dot{z}_k = -z_k|z_k|^2 + (\alpha + i\omega) z_k - \beta \sum_{j=1}^{N} (\kappa z_k - z_j), \tag{25}$$

where $i \in \{1, 2\}$. □

Remark 2: This reduction of the network of N units to a network of $N_R = 2$ units has the benefit of providing a characterization of different behaviors that the original network may exhibit.

Proof: Consider the matrices W and Q defined below (15). These matrices may also be expressed in function of the

two right eigenvectors v_1 and v_2 and the corresponding left eigenvectors, v_{l1} and v_{l2}, which in turn may be obtained by evaluating the pseudo-inverse $V_1^\dagger = (V_1^\top V_1)^{-1}V_1^\top$. We obtain

$$Q = \frac{1}{2}\begin{bmatrix} v_1 - v_2 & v_1 + v_2 \end{bmatrix}, \qquad W = \begin{bmatrix} v_{l1} - v_{l2} & v_{l1} + v_{l2} \end{bmatrix}.$$

Now, according to (15), $z_R = W^\top z$ and $z = Qz_R$. Therefore,

$$\dot{z}_R = W^\top F(z) + \beta W^\top \tilde{L} Q z_R, \tag{26}$$

with $\tilde{L} = \big[-L + \frac{\beta^*}{|\beta|^2}\Gamma \big]$.

Then, using the definitions of W and Q above, considering Assumption 1, and using the identities $v_{l1}^\top L = 0$ and $Lv_1 = 0$, we obtain

$$L_R := W^\top \mathcal{L} Q = \begin{bmatrix} 1 & -1 \\ -1 & 1 \end{bmatrix}.$$

On the other hand, we define

$$\Gamma_R := W^\top \Gamma Q = \begin{bmatrix} \tilde{\alpha} + i\tilde{\omega} & 0 \\ 0 & \tilde{\alpha} + i\tilde{\omega} \end{bmatrix}.$$

Hence, the second term on the right-hand side of (26) equals to $\gamma \tilde{L}_R z_R$, where

$$\tilde{L}_R = \big[-L_R + \frac{\beta^*}{|\beta|^2}\Gamma_R \big].$$

Next, we turn our attention to the first term on the right-hand side of (26). Since $z_R = W^\top z$, referring to (4), and defining $z_v = \begin{bmatrix} z_2^\top & z_3^\top & \cdots & z_N^\top \end{bmatrix}^\top$, we obtain

$$\dot{z}_R = \begin{bmatrix} \dot{z}_1 \\ \frac{1}{K}\mathbf{1}_K^\top \dot{z}_v, \end{bmatrix} = \begin{bmatrix} f(z_1) \\ \frac{1}{K}\sum_{k=2}^N f(z_k) \end{bmatrix} + \gamma \tilde{L}_R z_R.$$

Moreover, on $\{e = 0\}$ the relation $z_2 = z_3 = \cdots = z_N$ holds. Then $\frac{1}{K}\sum_{k=2}^N f(z_k) = \frac{1}{K}\sum_{k=2}^N f(z_2) = f(z_2)$. Thus, the reduced-order network takes the form

$$\dot{z}_R = \begin{bmatrix} f(z_1) \\ f(z_2) \end{bmatrix} + \gamma \tilde{L}_R z_R,$$

which is Equivalent to equations (25). ■

V. Effect of parameter mismatch

In this section, we focus on the effect of a disturbance on the oscillation frequency ω on the overall behavior of the network. More precisely, we assume that this $\delta\omega$ disturbance affects the 'leader' parameters. This translates into a transition to the dynamics

$$\dot{z}_1 = -z_1|z_1|^2 + \big[\alpha + i(\omega + \delta\omega)\big] z_1 + u_1 \tag{27a}$$
$$\dot{z}_k = -z_k|z_k|^2 + (\alpha + i\omega) z_k + u_k \tag{27b}$$

with u_k as introduced in (2) and $i \in \{2, 3, \cdots, N\}$. The network is heterogeneous since the first system's oscillation frequency is now $\omega + \delta\omega$. In the literature, analyzing the dynamics reduction of *heterogeneous* networks of oscillators when the coupling gain is low remains an open problem. For this reason, we assume in this section that $\mu = 0$ and $\kappa = 1$ (*i.e.* we analyze the behavior for a network with diffusive coupling). In compact form, (27) can be written as

$$\dot{z} = F(z) + \Gamma_2 z - \gamma L z \tag{28}$$

with

$$\Gamma_2 := \begin{bmatrix} \alpha + i(\omega + \delta\omega) & 0 \\ 0 & (\alpha + i\omega) I_{N-1}. \end{bmatrix}$$

In what follows, the collective behavior is analyzed as a function of two main parameters, the gain γ and the disturbance $\delta\omega$. As it may become clearer later, it is convenient to rewrite (5) as

$$\dot{z} = F(z) + \Gamma_2 z - \gamma \big[\mathcal{L} \otimes I_2\big] z, \tag{29}$$

where γ and $\mathcal{L}$ are scaled as follows:

$$\mathcal{L} = \frac{2}{\lambda_2(L)} L, \quad \gamma = \frac{\lambda_2(L)}{2}\bar{\gamma}. \tag{30}$$

Then, Eq. (5) becomes

$$\dot{z} = F(z) + \gamma \tilde{\mathcal{L}}_2 z, \tag{31}$$

where $\tilde{\mathcal{L}}_2 := \big[-\mathcal{L} + \frac{1}{\gamma}\Gamma_2 \big]$.

Now, in order to compare the behavior of the networked system before and after including the frequency perturbation, we rely on the following result for the unperturbed system. Note from Propositions 1-2 that the collective behavior of the network is characterized by a reduced-oder network of $N_R = 2$ oscillators, for $\beta > \beta_m = \gamma_m + i\mu_m$.

Proposition 3 ([1]): For the network (25), the in-phase solution is linearly asymptotically stable (*sic*), provided that

$$\gamma^2 + \mu^2 + \gamma[(1 - \kappa) + \alpha] > 0.$$

Otherwise, when

$$\gamma < \frac{\alpha}{4} \quad \text{and} \quad 3\gamma^2 - \alpha\gamma + \mu^2 > 0$$

the anti-phase solution is linearly asymptotically stable (*sic*). □

Remark 3: In [1] linear stability refers to local stability. Moreover, according to Proposition 2, on the synchronization manifold $\{e = 0\}$, the asymptotic behavior of the network (1)-(2) is represented by a network of $N_R = 2$ oscillators.

A. Eigenvalues of $\tilde{\mathcal{L}}$

To determine N_R we observe that under Assumption 1, $\mathcal{L}$ has a unique zero eigenvalue and admits the decomposition (8). Furthermore, note that

$$V^{-1}\Gamma_2 V = \begin{bmatrix} \alpha + i\omega + i\frac{\delta\omega}{2} & -i\frac{\delta\omega}{2} & 0 & \cdots & 0 \\ -i\frac{\delta\omega}{2} & \alpha + i\omega + i\frac{\delta\omega}{2} & 0 & \cdots & 0 \\ 0 & 0 & \alpha + i\omega & & 0 \\ 0 & 0 & 0 & \ddots & 0 \\ 0 & 0 & 0 & \cdots & \alpha + i\omega \end{bmatrix}.$$

As a result, the eigenvalues are given by

$$\lambda_1(\tilde{\mathcal{L}}_2) = -\lambda_2(\mathcal{L}) + \frac{2\alpha}{\gamma} + i(\omega + \frac{\delta\omega}{2}) - \frac{1}{2}\sqrt{\lambda_2(\mathcal{L})^2 - \frac{\delta\omega^2}{\gamma^2}}$$

$$\lambda_2(\tilde{\mathcal{L}}_2) = -\lambda_2(\mathcal{L}) + \frac{2\alpha}{\gamma} + i(\omega + \frac{\delta\omega}{2}) - \frac{1}{2}\sqrt{\lambda_2(\mathcal{L})^2 - \frac{\delta\omega^2}{\gamma^2}}$$

$$\lambda_k(\tilde{\mathcal{L}}_2) = -\lambda_k(\mathcal{L}) + \frac{2\alpha}{\gamma} + i\omega \qquad \text{for all } k \in \{3, 4, \cdots, N\}.$$

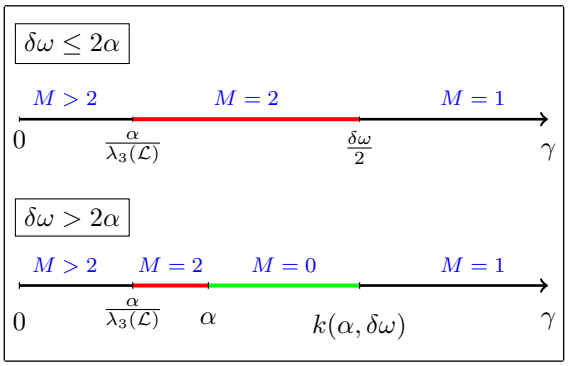

Fig. 1. Variations of M, the number of positive real part eigenvalues of the matrix $\tilde{\mathcal{L}}$ depending on the value of γ. Intervals in red are those where $M = 2$ and $k(\alpha, \delta\omega) := \frac{4\alpha^2+|\delta\omega|^2}{8\alpha}$.

Furthermore, the real part of $\lambda_k(\tilde{\mathcal{L}}_2)$for all $k \in \{3, 4, \cdots, N\}$ is given by $Re\{\lambda_k(\tilde{\mathcal{L}}_2)\} = -\lambda_k(\mathcal{L}) + \frac{2\alpha}{\gamma}$. The respective real part of the two first eigenvalues are

$$Re\{\lambda_1(\tilde{\mathcal{L}}_2)\} = -\lambda_2(\mathcal{L}) + \frac{2\alpha}{\gamma}$$
$$Re\{\lambda_2(\tilde{\mathcal{L}}_2)\} = -\lambda_2(\mathcal{L}) + \frac{2\alpha}{\gamma}$$

when $\gamma \leq \frac{\delta\omega}{\lambda_2(L)}$ and

$$Re\{\lambda_1(\tilde{\mathcal{L}}_2)\} = -\lambda_2(\mathcal{L}) + \frac{2\alpha}{\gamma} - \frac{1}{2}\sqrt{\lambda_2(\mathcal{L})^2 - \frac{\delta\omega^2}{\gamma^2}}$$
$$Re\{\lambda_2(\tilde{\mathcal{L}}_2)\} = -\lambda_2(\mathcal{L}) + \frac{2\alpha}{\gamma} - \frac{1}{2}\sqrt{\lambda_2(\mathcal{L})^2 - \frac{\delta\omega^2}{\gamma^2}}$$

when $\gamma > \frac{\delta\omega}{\lambda_2(\mathcal{L})}$. Let M be the number of eigenvalues of $\tilde{\mathcal{L}}_2$ with positive real part and note that $\lambda_2(\mathcal{L}) = 2$. Consequently, the sign of the real part of the two first eigenvalues of $\tilde{\mathcal{L}}_2$ depends on the parameters γ, $\delta\omega$ and α. We gather these two cases in the same figure by presenting the evolution of M in function of the gain γ.

The case of $M = 0$ corresponds to global asymptotic stability of the linear part $\dot{z} = \gamma\tilde{\mathcal{L}}z$. $M = 1$ brings us back to the known result of [9] on the practical stability of the set $\{z_1 = z_2 = \cdots = z_N\}$. In this paper, we focus on the case in which, given the relatively low values of the coupling gain γ, we have $M > 1$. It would, therefore, make sense for such a network to be modeled by a reduced network of $N_R = 2$ oscillators since it can also represent the first two behaviors previously explained ($M = 0$ and $M = 1$).

B. Behavior of the perturbed network

This section shows the effect of the $\delta\omega > 0$ perturbation on the whole network. In this configuration, for $\gamma > \frac{\alpha}{\lambda_3(\mathcal{L})}$, $\mathcal{L}$ has two eigenvalues with positive real parts. As a result, the definition of the synchronization error e is the same as in (13). So, even with the perturbation of the first oscillator frequency, the origin for the synchronization error $e = 0$ is globally asymptotically stable, and the proof follows with $\mathcal{V}(e) = e^*Pe$. Furthermore, the computations explained in the proof of Proposition 2 lead to the following result.

Proposition 4: Consider a network of N Stuart-Landau oscillators with dynamics (28) under Assumption 1. Then, on the synchronization manifold $\{e = 0\}$, if $\gamma > \frac{\alpha}{\lambda_3(\mathcal{L})}$, there exists a network of reduced order $N_R = 2$, whose nodes are dynamical systems of the form

$$\dot{z}_1 = -z_1|z_1|^2 + \Big(\alpha + i(\omega + \delta\omega)\Big)z_1 - \gamma(z_1 - z_2) \quad (32a)$$
$$\dot{z}_2 = -z_2|z_2|^2 + (\alpha + i\omega)z_1 - \gamma(z_2 - z_1). \quad (32b)$$

□

The following statement is reminiscent of Proposition 2.1 and Section 3 in [1], and characterizes the behavior of the reduced-order network when $\delta\omega > 0$. According to Proposition 4, for $\gamma > \frac{\alpha}{\lambda_3(\mathcal{L})}$, $\{e = 0\}$ is globally asymptotically stable and the collective behavior of the network is characterized by the reduced order network in (32), the statement follows.

Proposition 5: Consider a network of $N_R = 2$ Stuart-Landau oscillators with dynamics (32). Let $k(\alpha, \delta\omega) := \frac{\alpha^2+|\delta\omega|^2}{8\alpha}$, and $\gamma > \frac{\alpha}{\lambda_3(\mathcal{L})}$. Then,
if $\delta\omega > 2\alpha$,

1) the origin $\{z = 0\}$ is asymptotically stable, for all $\gamma \in \big]\alpha, k(\alpha, \delta\omega)\big[$;
2) if $\gamma \leq \alpha$, the network shows two trajectories with a phase drift, and,
3) if $\gamma \geq k(\alpha, \delta\omega)$, the network shows two trajectories with a phase lock.

If, otherwise, $\delta\omega \leq 2\alpha$,

4) the network shows two trajectories with a phase drift for all $\gamma < \frac{\delta\omega}{2}$ and
5) the network shows two trajectories with a phase lock for all $\gamma \geq \frac{\delta\omega}{2}$. □

□

For the initial homogeneous network, it can be seen that anti-phase solutions and the origin are unstable. Nevertheless, the perturbed network, over a given range of γ gain, can be stable at the origin. It is also noted that for the heterogeneous network, non-synchronization can appear in several possible forms: phase drift, where we see a time-varying phase difference, or phase lock, where oscillators are observed to adopt a fixed phase difference. The latter is less important as the coupling gain is increased and approaches zero when γ is very large. Although these results are linked to the coupling gain γ, they also depend on the amplitude of the disturbance $\delta\omega$.

VI. Numerical simulations

Consider a network of $N = 10$ Stuart-Landau oscillators interconnected according to a network with Laplacian L,

$$L = \begin{bmatrix} 1 & -1 & 0 & 0 & 0 & 0 & 0 & 0 & 0 & 0 \\ -1 & 1 & 0 & 0 & 0 & 0 & 0 & 0 & 0 & 0 \\ -1 & -2 & 3 & 0 & 0 & 0 & 0 & 0 & 0 & 0 \\ -1 & -2 & 0 & 3 & 0 & 0 & 0 & 0 & 0 & 0 \\ -1 & -2 & 0 & 0 & 3 & 0 & 0 & 0 & 0 & 0 \\ -1 & -2 & 0 & 0 & 0 & 3 & 0 & 0 & 0 & 0 \\ -1 & -2 & 0 & 0 & 0 & 0 & 3 & 0 & 0 & 0 \\ -1 & -2 & 0 & 0 & 0 & 0 & 0 & 3 & 0 & 0 \\ -1 & -2 & 0 & 0 & 0 & 0 & 0 & 0 & 3 & 0 \\ -1 & -2 & 0 & 0 & 0 & 0 & 0 & 0 & 0 & 3 \end{bmatrix},$$

and with $\alpha = 1$, $\omega = 2$, and $\kappa = 1$. This Laplacian L satisfies Assumption 1 since the first two eigenvecotors of L above satisfy exactly (6).

First, we consider the network to be homogeneous, i.e. $\delta\omega = 0$, and show the possibilities mentioned in Proposition 3. Figure 2 gives the trajectories of the network when the trajectories are in phase opposition.

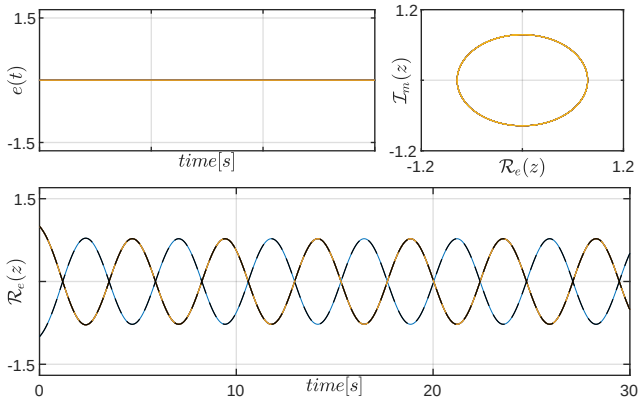

Fig. 2. Evolution of the trajectories of the homogeneous network with $\boldsymbol{\gamma = 0.2 + \frac{1}{3}i}$. The bottom plot corresponds to the anti-phase case and the dashed curves to the trajectories of the reduced-order network, the right-upper plot corresponds to the synchronization error. The left upper one corresponds to the phase plot of the trajectories.

The second full-synchronization case invoked in Proposition 3 is shown in Figure 3, below.

In a second step, we introduce a $\delta\omega$ perturbation in the frequency of the first oscillator and show the effect of these perturbations through different values of $\delta\omega$ as well as γ, such that each behavior invoked in Proposition 5 is depicted. Furthermore, after Proposition 5, when the perturbation satisfies $\delta\omega > 2\alpha = 2$ and $\gamma \in]\frac{\alpha}{\lambda_3(\mathcal{L})}, \alpha]$, the trajectories show a phase drift, depicted in Figure 5. Moreover, after the same proposition, if $\gamma \geq k(\alpha, \delta\omega)$, the network shows two trajectories with a phase lock, this can be noticed in Figure 6. Next, we show the behavior of the network when the frequency perturbation satisfies $\delta\omega \leq 2\alpha = 2$. The phase-drift and phase-lock invoked in Proposition 5 are shown in Figures 7-8.

VII. Conclusion

This paper presents results on the reduction of connected oscillator networks based on the spectral properties of interconnection matrices. The results show, first, that it is possible

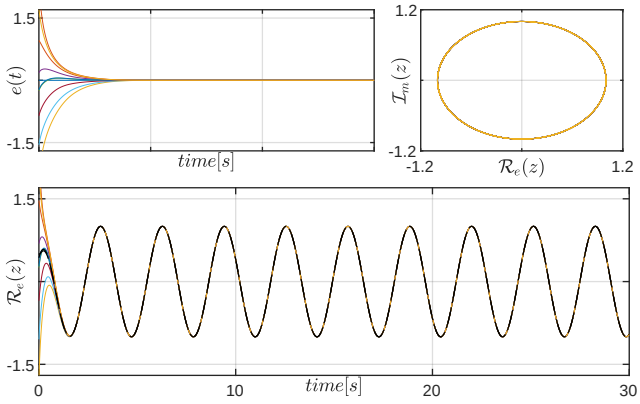

Fig. 3. Evolution of the trajectories of the homogeneous network with $\boldsymbol{\gamma = 1 + 0.5i}$. The bottom plot corresponds to the anti-phase case and the dashed curves to the trajectories of the reduced-order network,, the right-upper plot corresponds to the synchronization error. The left upper one corresponds to the phase plot of the trajectories.

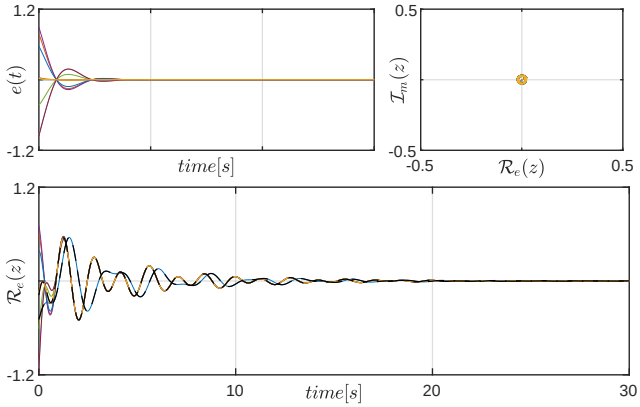

Fig. 4. Numerical results for $\boldsymbol{\delta\omega = 3}$ and $\boldsymbol{\gamma = 1.2}$, the dashed black curves stand for the trajectories of the reduced order network. After a short transient, the behavior of the initial network is identical to the behavior of the reduced order network, which explains the superposition of the curves. This remark is supported by the global asymptotic stability of $\boldsymbol{e = 0}$.

to reduce the network of N oscillators to a reduced network of $N_R < N$ oscillators while preserving the collective behavior of the network. This advantage then allows the analysis of the different collective behaviors that can be observed, as well as the effect of a disturbance on network synchronization. Future research will focus on further generalizing the application of this reduction method.

References

[1] D. Aronson, G. Ermentrout, and N. Kopell, "Amplitude response of coupled oscillators," *Physica D: Nonlinear Phenomena*, vol. 41, no. 3, pp. 403–449, 1990.

[2] P. C. Matthews and S. H. Strogatz, "Phase diagram for the collective behavior of limit-cycle oscillators," *Phys. Rev. Lett.*, vol. 65, pp. 1701–1704, Oct 1990.

[3] P. C. Matthews, R. E. Mirollo, and S. H. Strogatz, "Dynamics of a large system of coupled nonlinear oscillators," *Physica D: Nonlinear Phenomena*, vol. 52, no. 2, pp. 293–331, 1991.

[4] G. Ermentrout, "Oscillator death in populations of "all to all" coupled nonlinear oscillators," *Physica D: Nonlinear Phenomena*, vol. 41, no. 2, pp. 219–231, 1990.

[5] M. Soriano, J. Garcia-Ojalvo, C. Mirasso, and I. Fischer, "Complex photonics: Dynamics and applications of delay-coupled semiconductors lasers," *Review of Modern Physics*, vol. 85, p. 421, 03 2013.

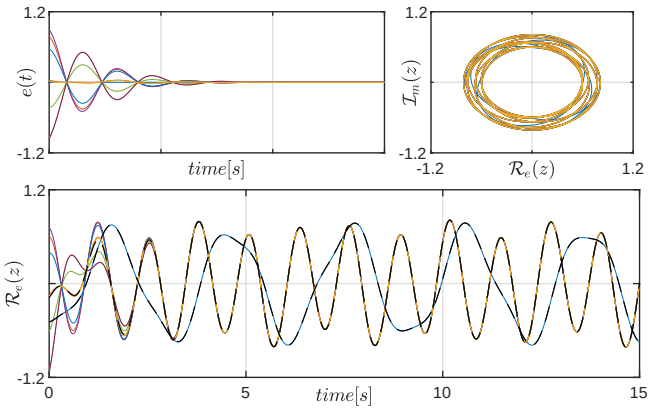

Fig. 5. Numerical results for $\boldsymbol{\delta\omega = 3}$ and $\boldsymbol{\gamma = 0.5}$, the dashed black curves stand for the trajectories of the reduced order network. After a short transient, the behavior of the initial network is identical to the behavior of the reduced order network, which explains the superposition of the curves. This remark is supported by the global asymptotic stability of $\boldsymbol{e = 0}$.

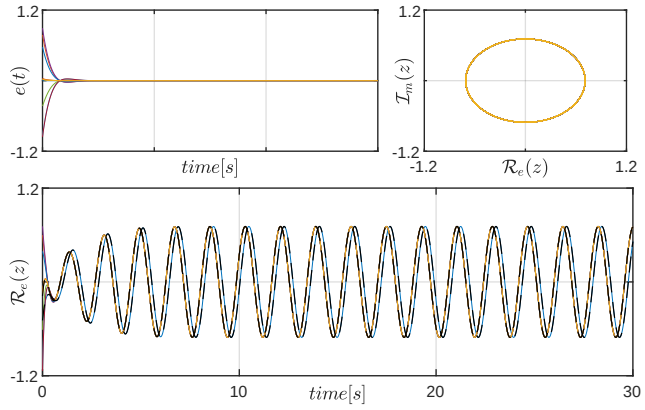

Fig. 6. Numerical results for $\boldsymbol{\delta\omega = 3}$ and $\boldsymbol{\gamma = 2.5}$, the dashed black curves stand for the trajectories of the reduced order network. After a short transient, the behavior of the initial network is identical to the behavior of the reduced order network, which explains the superposition of the curves. This remark is supported by the global asymptotic stability of $\boldsymbol{e = 0}$.

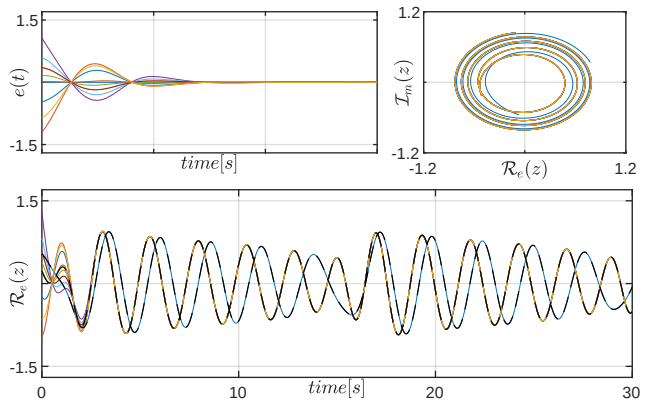

Fig. 7. Numerical results for $\boldsymbol{\delta\omega = 1}$ and $\boldsymbol{\gamma = 0.45}$, the dashed black curves stand for the trajectories of the reduced order network. After a short transient, the behavior of the initial network is identical to the behavior of the reduced order network, which explains the superposition of the curves.

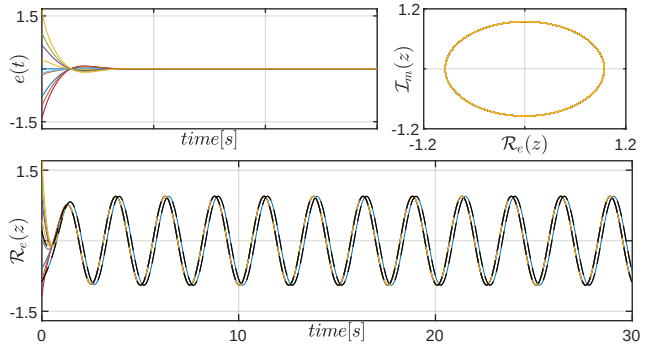

Fig. 8. Numerical results for $\boldsymbol{\delta\omega = 1}$ and $\boldsymbol{\gamma = 2.5}$, the dashed black curves stand for the trajectories of the reduced order network. After a short transient, the behavior of the initial network is identical to the behavior of the reduced order network, which explains the superposition of the curves.

[6] V. Vlasov and A. Bifone, "Hub-driven remote synchronization in brain networks," *Scientific Reports*, vol. 7, 12 2017.

[7] L. Kang, Z. Wang, S. Huo, C. Tian, and Z. Liu, "Remote synchronization in human cerebral cortex network with identical oscillators," *Nonlinear Dynamics*, vol. 99, 01 2020.

[8] J. Hasty, D. Mcmillen, F. Isaacs, and J. Collins, "Computational studies of gene regulatory networks: In numero molecular biology," *Nature reviews. Genetics*, vol. 2, pp. 268–79, 05 2001.

[9] E. Panteley, A. Loría, and A. El-Ati, "Practical dynamic consensus of Stuart-Landau oscillators over heterogeneous networks," *Int. J. of Control*, vol. 93, no. 2, pp. 261–273, 2020.

[10] G. Vathakkatil Joseph and V. Pakrashi, "Limits on anti-phase synchronization in oscillator networks," *Scientific Reports*, vol. 10, p. 10178, 06 2020.

[11] M. Frasca, A. Bergner, J. Kurths, and L. Fortuna, "Bifurcations in a star-like network of stuart-landau oscillators," *Int. J. Bifurc. Chaos*, vol. 22, 2012.

[12] Z. Zheng, X.-q. Feng, B. Ao, and M. Cross, "Synchronization on coupled dynamical networks," *Frontiers of Physics in China*, vol. 1, pp. 458–467, 01 2006.

[13] M. T. Schaub, N. O'Clery, Y. N. Billeh, J.-C. Delvenne, R. Lambiotte, and M. Barahona, "Graph partitions and cluster synchronization in networks of oscillators," *Chaos: An Interdisciplinary Journal of Nonlinear Science*, vol. 26, no. 9, p. 094821, 2016.

[14] L. Tumash, E. Panteley, A. Zakharova, and E. Schöll, "Synchronization patterns in stuart–landau networks: a reduced system approach," *The European Physical Journal B*, vol. 92, 05 2019.

[15] M. Rosenblum, A. Pikovsky, and J. Kurths, "Phase synchronization of chaotic oscillators," *Physical review letters*, vol. 76, pp. 1804–1807, 04 1996.

[16] A. Nazerian, S. Panahi, and F. Sorrentino, "Synchronization in networks of coupled oscillators with mismatches," *Europhysics Letters*, vol. 143, no. 1, p. 11001, jul 2023.

[17] S. Jalan, A. Singh, S. Acharyya, and J. Kurths, "Impact of leader on cluster synchronization," *Physical Review E*, vol. 91, p. 022901, 02 2015.

[18] R. Parker and A. K. Barreiro, "Bifurcations of a neural network model with symmetry," *SIAM Journal on Applied Dynamical Systems*, vol. 21, no. 4, pp. 2535–2578, dec 2022.

[19] A. S. Powanwe and A. Longtin, "Amplitude-phase description of stochastic neural oscillators across the hopf bifurcation," *Phys. Rev. Res.*, vol. 3, p. 033040, Jul 2021.

[20] R. Gast, S. A. Solla, and A. Kennedy, "Macroscopic dynamics of neural networks with heterogeneous spiking thresholds," *Phys. Rev. E*, vol. 107, p. 024306, Feb 2023.

[21] F. Liljeros, C. R. Edling, and L. A. Amaral, "Sexual networks: implications for the transmission of sexually transmitted infections," *Microbes and Infection*, vol. 5, no. 2, pp. 189–196, 2003.

[22] B.-H. Avner, B. Pierre, and D. Sophie, "Block models for generalized multipartite networks applications in ecology and ethnobiology," *Statistical Modelling*, vol. 22, no. 4, pp. 273–296, 2022.

[23] J. Lacerda, C. Freitas, and E. Macau, "Multistable remote synchronization in a star-like network of non-identical oscillators," *Applied Mathematical Modelling*, vol. 69, pp. 453–465, 2019.

[24] H. Kitajima and J. Kurths, "Bifurcation in neuronal networks with hub structure," *Physica A: Statistical Mechanics and its Applications*, vol. 388, no. 20, pp. 4499–4508, 2009.

[25] E. Panteley and A. Loría, "Synchronization and dynamic consensus of heterogeneous networked systems," *IEEE Trans. on Automatic Control*, vol. 62, no. 8, pp. 3758–3773, 2017.